

A Non-Electrostatic Surface Complexation Approach to Modeling Radionuclide Migration: The Role of Iron Oxides and Carbonates

M. Zavarin, C.J. Bruton

This paper was prepared for submittal to the
Migration '99, Seventh International Conference
Incline Village, Nevada, September 26 – October 1, 1999

U.S. Department of Energy

Lawrence
Livermore
National
Laboratory

September 20, 1999

DISCLAIMER

This document was prepared as an account of work sponsored by an agency of the United States Government. Neither the United States Government nor the University of California nor any of their employees, makes any warranty, express or implied, or assumes any legal liability or responsibility for the accuracy, completeness, or usefulness of any information, apparatus, product, or process disclosed, or represents that its use would not infringe privately owned rights. Reference herein to any specific commercial product, process, or service by trade name, trademark, manufacturer, or otherwise, does not necessarily constitute or imply its endorsement, recommendation, or favoring by the United States Government or the University of California. The views and opinions of authors expressed herein do not necessarily state or reflect those of the United States Government or the University of California, and shall not be used for advertising or product endorsement purposes.

This is a preprint of a paper intended for publication in a journal or proceedings. Since changes may be made before publication, this preprint is made available with the understanding that it will not be cited or reproduced without the permission of the author.

This report has been reproduced
directly from the best available copy.

Available to DOE and DOE contractors from the
Office of Scientific and Technical Information
P.O. Box 62, Oak Ridge, TN 37831
Prices available from (423) 576-8401
<http://apollo.osti.gov/bridge/>

Available to the public from the
National Technical Information Service
U.S. Department of Commerce
5285 Port Royal Rd.,
Springfield, VA 22161
<http://www.ntis.gov/>

OR

Lawrence Livermore National Laboratory
Technical Information Department's Digital Library
<http://www.llnl.gov/tid/Library.html>

Migration 99 - Radiochimica Acta
Mavrik Zavarin* and Carol J. Bruton
Lawrence Livermore National Laboratory
7000 East Avenue, L-219
Livermore, CA 94551

9/20/99

* phone: (925) 424-6491; email: zavarin1@llnl.gov

Keywords: carbonates, iron oxides, sorption, modeling, surface complexation

A Non-Electrostatic Surface Complexation Approach to Modeling Radionuclide Migration: The Role of Iron Oxides and Carbonates

Summary

Reliable quantitative prediction of contaminant transport in sub-surface environments is critical to evaluating the risks associated with radionuclide migration. A non-electrostatic surface complexation (NEM SC) approach to radionuclide sorption in conjunction with existing ion exchange models is being used in near-field reactive transport simulations at the Nevada Test Site (NTS). Published radionuclide sorption data were fit to NEM SC reactions and a reaction database was developed for use in reactive transport simulations. For radionuclide-iron oxide sorption, one-site NEM SC reactions adequately fit most data without need for bidentate or ternary surface species. For example, the decrease in U(VI) sorption as a function of carbonate alkalinity was accounted for by aqueous uranyl-carbonate complex formation. Calcite reactions were modeled as NEM surface exchange reactions. Reactive transport simulations using the NEM SC database suggest that migration of Sm, Eu, Np, Pu, and Am will be significantly retarded by sedimentary carbonates. Though iron oxides are usually thought to be the major contributors to radionuclide retardation, carbonates will also be of paramount importance in areas where they are present.

Introduction

Sorbing minerals (e.g. goethite, calcite) can significantly reduce radionuclide (RN) mobility in the environment. Radionuclide sorption can be described by surface complexation (SC)¹ reactions of the form:



¹ Processes such as ion exchange and precipitation can also contribute to RN retardation but are not discussed here.

$$K = \frac{(> \text{FeOSr}^+)(\text{H}^+)}{(> \text{FeOH})(\text{Sr}^{2+})} \quad (2)$$

where $>\text{FeOH}$ is a functional group on the surface of iron oxide and Sr^{2+} is an aqueous strontium species that sorbs onto the surface to form $>\text{FeOSr}^+$. The equilibrium constant K describes the relative activity of all species at equilibrium.

Partitioning K_d values, typically reported as a ratio of total sorbed concentration (mol/g) to total aqueous concentration (mol/ml), are often used to model sorption. Though RN sorption to a sediment or mineral at a specific pH and solution composition can be adequately described using the K_d approach, the approach does not typically account for sorptive changes in chemically and mineralogically varying geologic environments. The SC approach is not limited in this way because sorption is defined as a function of solution chemistry and mineral reactive site concentration. Thus, the SC approach provides a much more robust basis for simulating RN reactive transport in environments where water chemistry and mineralogy may change.

Although there are many models that describe SC (constant capacitance, diffuse layer, triple layer, and others), the non-electrostatic model (NEM) (1) contains the fewest fitting parameters. Unlike other SC models, the NEM assumes that electrical charge at mineral surfaces does not affect SC. Thus, the activity of a surface species is equal to its concentration. Although the NEM oversimplifies SC, several investigators have used this approach to describe sorption (2, 3, 4). Davis et al. (3) argued that the NEM may be the most appropriate model for complex environmental applications because the surface charging behavior of non-ideal natural mineral phases is not well known. Below, we describe the NEM SC approach used in RN reactive transport simulations away from underground nuclear tests at the Nevada Test Site (NTS) (5).

Methods

A NEM SC database was compiled by fitting published sorption data. Selection criteria for RNs were based on abundance, half-life, toxicity to human and environmental health, and potential mobility at NTS (5). The minerals of interest were chosen based on their reactivity and abundance at NTS; RN sorption to iron oxides and carbonates is discussed in this paper. Sorption data was

fit using the computer program FITEQL (6). Ionic strength, pH, and aqueous complexation were taken into account during fitting while surface electrostatic effects were neglected. The aqueous species used to fit the data were based on the GEMBOCHS thermodynamic data base version data.com.V8.R6 (7) with revisions as noted in (5). All sorption data for iron oxides and carbonates were fit with a one-site model and the minimum number of surface species required for an adequate fit. Sorption data of iron oxides are typically fit with a two-site model in which weak and strong sorbing sites contribute to sorption (8). The calcite surface is also thought to have non-uniform surface complexation sites (9). The one-site model was used, in this case, to examine whether a minimum number of fitting parameters could adequately fit the majority of published sorption data.

Iron oxide NEM SC constants were calculated from a combination of hydrous ferric oxide, goethite, and hematite sorption data. Sorption data for the various iron oxides was consolidated by accounting for surface area differences while assuming that surface functional groups behave identically. When the published data did not include surface areas, 600 m²/g was assumed for hydrous ferric oxide and 50 m²/g for goethite. The site density for all iron oxides was assumed to be 2.31 sites/nm² (10). In cases where hydrous ferric oxide concentrations were reported as mol-Fe/L, the reactive site concentration was assumed to be 0.205 mol sites/mol Fe. This site density is equal to the sum of strong and weak sites as described by Dzombak and Morel (8) for hydrous ferric oxide.

Sorption reaction constants for carbonates were determined using only calcite sorption data. A site density of 10.8 sites/nm² (or 1.8*10⁻⁵ mol/m²), in combination with BET surface area, was used to determine the reactive site concentration. This value was suggested by Zachara et al. (11) based on Ca isotopic exchange measurements. Along the 1014 plane of calcite, the Ca density is ~50% less than the value reported by Zachara et al. (11). Sorption may occur within a hydrated calcite surface layer that is several monolayers thick. It is therefore possible that the effective number of surface “sorption” sites is greater than the maximum number of surface Ca positions. Unlike iron oxide SC reactions, calcite reactions were written as surface exchange reactions.

Cations may bind directly to exposed $>CO_3$ surface sites. However, it is assumed here, in accordance with previous calcite sorption studies, that cations sorb by exchange with Ca (11, 12, 13, 14, 15).

When multiple sorption data sets were available, NEM SC database constants were determined from an average of the most reliable data. In some cases, SC constants were chosen to yield a conservative estimate of sorption.

Reactive transport simulations used to compare the sorptive behavior of calcite and iron oxides were performed using the **Global Implicit Multicomponent Reactive Transport (GIMRT)** code (16). Simulations were run using a sediment mineralogy equivalent to that used in recent near-field reactive transport simulations in Frenchman Flat, NTS, alluvium (5). Iron oxide surface area and site density were $50 \text{ m}^2/\text{g}$ and $2.31 \text{ sites}/\text{nm}^2$, respectively. Calcite surface area and site density were $2.2 \text{ m}^2/\text{g}$ and $8.31 \times 10^{-6} \text{ mol}/\text{m}^2$ (a conservative estimate), respectively (13).

Results and Discussion

A. Iron Oxide as Sorbent

Table 1 contains the average iron oxide NEM SC constants determined from fitting published data. Surface acidity constants for iron oxide were taken from Dzombak and Morel (8).² Generic iron oxide NEM SC reactions adequately fit most published data. There was no need to add more complex bidentate or ternary surface complexes or differentiate between the various iron oxide minerals (e.g. Fig. 1). However, a one-site model could not always fit sorption at both high and low surface loads (e.g. Fig. 2). The change in sorption affinity at high Sr and Eu surface loads (data of Kolarik (17) and Rabung et al. (18), respectively) is indicative of sorption to multiple sites and possible electrostatic effects (e.g. Dzombak and Morel (8)). A change in sorption affinity with increasing surface load was not detected in U(VI) sorption data; U(VI) sorption data from trace up to near saturation loads were fit adequately using the one-site NEM. High surface loading is expected to be a rare occurrence at NTS, though the failure of the one-site NEM at high Sr and Eu

² Acidity constants vary depending on both the iron oxide mineral and the SC model (e.g. diffuse layer $\log K_+$ and $\log K_-$ constants of 6.7 to 7.4 and -6.4 to -9.2, respectively, for several iron oxide minerals (10)). The diffuse layer hydrous ferric oxide surface acidity constants were used in this generic iron oxide NEM SC database for convenience.

surface loads is an indication of the limitations of the approach. All Np(V), Pu(IV), and Pu(V) sorption data examined had relatively low surface loads (<10%) and fit well using the one-site NEM. The Np(V) and Pu(V) NEM SC constants are similar which would be expected given their similar electronic configuration and aqueous complexation behavior. The observation that Pu(IV) dominates over Pu(V) on iron oxide surfaces (19, 20, 21) can be attributed to the higher sorption affinity of Pu(IV) (Fig. 3).

When iron oxides interact with groundwater, some surface sites are likely to be occupied by Ca, Mg, CO₃, SO₄, PO₄, Si(OH)₄, and other ions. Previous calculations using NTS porewater composition indicated that the iron oxide surface sites will not be saturated by groundwater ions (5). It was also estimated that the RN concentrations would be low enough not to occupy a significant portion of the available surface sites. Thus, competition between RNs and groundwater ions for surface sites did not occur in our first NTS simulations (5). In U(VI)-goethite SC data fits, the change in sorption as a function of carbonate alkalinity did not result from competition between carbonate and U(VI) for surface sites or from ternary surface complexation reactions. The decrease in sorption as a function of carbonate alkalinity could be attributed to aqueous uranyl-carbonate complexation (Fig. 4).

B. Calcite as Sorbent

Although there is large amount of information available on the sorptive properties of carbonates for divalent cations (11, 15), the sorption of actinides and lanthanides on carbonates is less well known. Nevertheless, the available information suggests that calcite can be an important sorbent for certain elements. For example, Keeney-Kennicutt and Morse (22) observed that Np(V) affinity for mineral surfaces, on a mineral surface area basis, was as follows: aragonite ≥ calcite > goethite > MnO₂ ≈ clays (pH ~8 solutions). Keeney-Kennicutt and Morse (21) also observed that, on a mineral surface area basis, Pu(V) sorbs to calcite only slightly less than to goethite (pH ~8 solutions).

Table 2 lists the average calcite NEM SC constants determined from fitting published data.

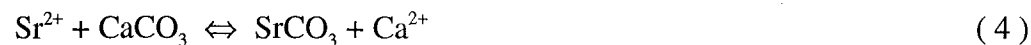
Sorption data was available only at pH~8 for Am(III), Eu(III), Np(V), Pu(V), and Sm(III). If reactive transport simulations deviate significantly from pH~8, the uncertainty associated with the resulting sorption values will be large. Nevertheless, because the pH of groundwater at the NTS is typically near 8, the SC constants listed in Table 2 are a reasonable estimate of RN sorption to calcite in this area. Additional sorption data over a range of pH and solution composition is critical to improving reactive transport simulations in calcareous environments.

For Am(III), Eu(III), and Sm(III), the dominant positively charged aqueous species in solution at pH~8 and in equilibrium with atmospheric CO₂(g) (i.e. the mono-carbonate species) was chosen as the sorbing species. The choice of sorbing species could not be constrained because information regarding sorption as a function of pH or alkalinity was not available. The mono-carbonate species was chosen to ensure that deviations in pH from 8 would not radically increase sorption. The logK values for all three trivalent cations are relatively similar. Differences in logK are related to changes in aqueous speciation as well as sorptive behavior. The SC constants are strictly dependent on aqueous speciation and the associated reaction constants. The logK values in this paper are, thus, valid only when used in conjunction with the aqueous species and thermodynamic constants used to derive the SC database.

Both sorption and coprecipitation data were available for Sm(III) and Eu(III). Trace element sorption data can be related to coprecipitation data through the Doerner-Hoskins rule (23). The Doerner-Hoskins rule states that coprecipitation partitioning can be described as continuous surface monolayer equilibrium partitioning. The surface reaction:



is equivalent to the coprecipitation partitioning reaction



when $>\text{Ca}^{2+}$ and $>\text{Sr}^{2+}$ are expressed as mole fractions of surface species and CaCO₃ and SrCO₃ as mole fractions of solid solution components. Total elemental concentrations in solution are typically used to evaluate partitioning coefficients; here, we use the activity of aqueous species.

The fits to Sm(III), Eu(III), La(III), and Yb(III) data are listed in Table 3. Although the logK values for sorption and coprecipitation are not identical, they are in general agreement. The more conservative logK values were selected for the NEM SC database (Table 2). Coprecipitation logK values of Sm and Eu were the most conservative.

For Np(V) and Pu(V), the positively charged aqueous species NpO_2^+ and PuO_2^+ were assumed to be the sorbing species. The logK values for these two sorption reactions are similar, as expected. The logK for Np(V) listed in Table 2 was compared with Np(V) sorption data of Triay et al. (24). Triay et al. (24) conducted batch sorption studies in synthetic J-13 and UE-25 p#1 waters from Yucca Mountain, Nevada, which are similar in composition to those found at NTS. Single-point logK values were determined from raw data reported by Triay et al. (24) and aqueous speciation calculations using the REACT[®] program (25). For reactions lasting 21 to 31 days, logK values varied between 0.6 and 2.8 while the average and standard deviation of all measurements equaled 0.7 and 0.9, respectively. Reported K_d values varied from 800 to 1 ml/g. The large variability of logK illustrates the difficulty in measuring carbonate SC constants. Calcite surfaces are unstable and can undergo dissolution, precipitation, recrystallization, and solid state diffusion reactions which makes sorption quantification difficult. Nevertheless, the long-term reaction constants calculated from the data of Triay et al. (24) are in agreement with the average logK listed in Table 2.

The SC constant for Sr(II) was determined using available pH dependent sorption data. The SC constant for U(VI) was taken directly from the results of Carroll and Bruno (14); their data were presented in the same surface exchange format listed in Table 2. The small logK value determined here for Sr(II) agrees with published partitioning values (11, 15). Though the U(VI) logK value is large, sorption to calcite is very weak (14). The large logK value results from U(VI) aqueous speciation at pH>5, which is typically dominated by mono-, di-, and tri-carbonate species rather than UO_2^{++} .

C. Comparison of Radionuclide Sorption to Carbonates and Iron Oxides

The influence of carbonates and iron oxides on RN migration was examined with the reactive

transport GIMRT code (16). The alluvium mineralogy and uncontaminated groundwater composition was the same as in the simulations reported by Tompson et al. (5). In the following simulations, total RN concentrations were set at a low enough value such that precipitation would not occur. In addition to the SC constants described above, ion exchange of Sr on clinoptilolite and smectite was described using data and models from Viani and Bruton (26, 27) as discussed in (5).

For Np, Eu, and Pu, both calcite and iron oxide contributed significantly to RN sorption (Table 4). The combination of iron oxide and calcite in the alluvium reduced the Eu, Np, and Pu concentrations in the simulated groundwater by about 4, 3, and 2 orders of magnitude, respectively. About 10% of the sorbed Np and Pu and 50% of the sorbed Eu was associated with carbonates. The concentration of aqueous Pu remained somewhat high. The groundwater composition in this simulations was highly oxidic (dominated by Pu(V)); if Pu(IV) were present in significant amounts, Pu would sorb to a much greater extent. Am(III) and Sm(III) sorption to carbonates reduced the aqueous concentration by over 4 and nearly 3 orders of magnitude, respectively. Sorption of these cations to iron oxides was not evaluated for lack of data.

U and Sr did not sorb significantly to calcite. U(VI) sorption to iron oxides controlled the aqueous U(VI) concentration; U(VI) associated with calcite was ~5 orders of magnitude less than with iron oxide. For Sr, ion exchange with clinoptilolite and smectite controlled the aqueous Sr(II) concentration; only ~1% of Sr(II) was associated with iron oxide and 0.01% was associated with calcite.

This work was conducted under the auspices of the U. S. Department of Energy by Lawrence Livermore National Laboratory under contract W-7405-Eng-48. This work was funded by the Underground Test Area Project, U. S. Department of Energy, Nevada Operations Office.

References

1. M. H. Kurbatov, G. B. Wood, J. D. Kurbatov: *J. Phys. Chem.* **55**, 1170 (1951).
2. J. M. Zachara, C. T. Resch, S. C. Smith: *Geochim. Cosmochim. Acta* **58**, 553 (1994).
3. J. A. Davis, J. A. Coston, D. B. Kent, C. C. Fuller: *Environ. Sci. Technol.* **32**, 2820

- (1998).
4. M. H. Bradbury, B. Baeyens: *J. Contam. Hydrol.* **27**, 223 (1997).
 5. A. F. B. Tompson, C. J. Bruton, G. A. Pawloski: Evaluation of the Hydrologic Source Term from the Underground Nuclear Tests in Frenchman Flat and the Nevada Test Site: The CAMBRIC Test, UCRL-ID-132300, Lawrence Livermore National Laboratory (1999).
 6. A. L. Herbelin, J. C. Westall: FITEQL: A Computer Program for Determination of Chemical Equilibrium Constants from Experimental Data, Department of Chemistry, Oregon State University (1994).
 7. J. W. Johnson, S. R. Lundeen: GEMBOCHS Thermodynamic Datafiles for Use with the EQ3/6 Modeling Package, Lawrence Livermore National Laboratory (1997).
 8. D. A. Dzombak, F. M. M. Morel: *Surface Complexation Modeling : Hydrous Ferric Oxide*, Wiley, New York (1990).
 9. C. E. Cowan, J. M. Zachara, C. T. Resch: *Geochim. Cosmochim. Acta* **54**, 2223 (1990).
 10. D. R. Turner: A Uniform Approach to Surface Complexation Modeling of Radionuclide Sorption, CNWRA 95-001, Center for Nuclear Waste Regulatory Analyses (1995).
 11. J. M. Zachara, C. E. Cowan, C. T. Resch: *Geochim. Cosmochim. Acta* **55**, 1549 (1991).
 12. J. M. Zachara, J. A. Kittrick, J. B. Harsh: *Geochim. Cosmochim. Acta* **52**, 2281 (1988).
 13. J. M. Zachara, C. E. Cowan, C. T. Resch, *Metals in Groundwater*, H. E. Allen, E. M. Perdue, D. S. Brown, Eds., Lewis Publishers, Boca Raton (1993), Chap. 2.
 14. S. A. Carroll, J. Bruno: *Radiochim. Acta* **52-3**, 187 (1991).
 15. H. E. Doner, M. Zavarin: *Soils And Environment : Soil Processes from Mineral to Landscape Scale*, K. Auerswald, J. M. Bigham, H. Stanjek, Eds., Catena Verlag, Reiskirchen, Germany (1997), pp. 407-422.
 16. C. I. Steefel, S. B. Yabusaki, OS3D/GIMRT: Software for Modeling Multicomponent-Multidimensional Reactive Transport, Pacific Northwest National Laboratory, Richland, Washington (1995).

17. Z. Kolarik: Collection Czech. Chem. Commun. **27**, 938 (1961).
18. T. Rabung, H. Geckeis, J. Kim, H. P. Beck: J. Coll. Interf. Sci. **208**, 153 (1998).
19. A. L. Sanchez: Ph.D. Dissertation, University of Washington (1983).
20. A. L. Sanchez, J. W. Murray, T. H. Sibley: Geochim. Cosmochim. Acta **49**, 2297 (1985).
21. W. L. Keeney-Kennicutt, J. W. Morse: Geochim. Cosmochim. Acta **49**, 2577 (1985).
22. W. L. Keeney-Kennicutt, J. W. Morse: Marine Chem. **15**, 133 (1984).
23. W. Stumm: *Chemistry of the Solid-Water Interface*, John Wiley and Sons, Inc., New York, (1992), Appendix A.6.2.
24. I. R. Triay, et al.: Batch Sorption Results for Neptunium Transport Through Yucca Mountain Tuffs, LA-12961-MS, Los Alamos National Laboratory (1996).
25. C. M. Bethke: *Geochemical Reaction Modeling: Concepts and Applications*, Oxford University Press, New York (1996).
26. B. E. Viani, C. J. Bruton: Modeling Fluid-Rock Interaction at Yucca Mountain, Nevada: A Progress Report, UCRL-ID-109921, Lawrence Livermore National Laboratory (1992).
27. B. E. Viani, C. J. Bruton: Assessing the Role of Cation Exchange in Controlling Groundwater Chemistry During Fluid Mixing in Fractured Granite At Aspo, Sweden, UCRL-JC-121527, Lawrence Livermore National Laboratory (1996).
28. T. Fujita, M. Tsukamoto: Material Research Society, **465**, 781 (1997).
29. A. Ledin, S. Karlsson, A. Duker, B. Allard: Radiochim. Acta **66-7**, 213 (1994).
30. D. C. Girvin, L. L. Ames, A. P. Schwab, J. E. McGarrah: J. Colloid Interface Sci. **141**, 67 (1991).
31. S. Nakayama, Y. Sakamoto: Radiochim. Acta **52-3**, 153 (1991).
32. D. G. Kinniburgh, J. K. Syers, M. L. Jackson: Soil Sci. Soc. Am. J. **39**, 464 (1975).
33. M. C. Duff, C. Amrhein: Soil Sci. Soc. of Am. J. **60**, 1393 (1996).
34. B. E. Viani, P. C. Torretto: Sorption and Transport of Uranium on Hematite, Milestone SPL3BM4, UCRL-ID-19848, Lawrence Livermore National Laboratory, (1998).

35. C. D. Hsi, D. Langmuir: *Geochim. Cosmochim. Acta* **49**, 1931 (1985).
36. T. D. Waite, J. A. Davis, T. E. Payne, G. A. Waychunas, N. Xu: *Geochim. Cosmochim. Acta* **58**, 5465 (1994).
37. P. M. Shanbhag, J. W. Morse: *Geochim. Cosmochim. Acta* **46**, 241 (1982).
38. S. J. Zhong, A. Mucci: *Geochim. Cosmochim. Acta* **59**, 443 (1995).

Table 1. Surface complexation reactions for iron oxides using the NEM

Reaction	# of Curves Evaluated	logK	Ref.
$>\text{FeOH} \Leftrightarrow \text{FeO}^- + \text{H}^+$		-8.93	(10)
$>\text{FeOH} + \text{H}^+ \Leftrightarrow \text{FeOH}_2^+$		7.29	
$>\text{FeOH} + \text{Eu}^{3+} \Leftrightarrow >\text{FeOEu}^{2+} + \text{H}^+$	11	1.87 ± 0.69	(18, 28, 29)
$>\text{FeOH} + \text{Eu}^{3+} + \text{H}_2\text{O} \Leftrightarrow >\text{FeOEuO} + 3\text{H}^+$		-13.74 ± 0.17	
$>\text{FeOH} + \text{NpO}_2^+ \Leftrightarrow >\text{FeOHNpO}_2^+$	10	4.32 ± 0.11	(30, 31)
$>\text{FeOH} + \text{NpO}_2^+ + \text{H}_2\text{O} \Leftrightarrow >\text{FeOHNpO}_3^- + 2\text{H}^+$		-11.26	
$>\text{FeOH} + \text{Pu}^{4+} + \text{H}_2\text{O} \Leftrightarrow >\text{FeOHPuO}_2^{2+} + 2\text{H}^+$	2	6.93	(20)
$>\text{FeOH} + \text{Pu}^{4+} + 2\text{H}_2\text{O} \Leftrightarrow >\text{FeOHPuO}_2 + 4\text{H}^+$		-1.29	
$>\text{FeOH} + \text{PuO}_2^+ \Leftrightarrow >\text{FeOHPuO}_2^+$	2	4.79	(20)
$>\text{FeOH} + \text{PuO}_2^+ + \text{H}_2\text{O} \Leftrightarrow >\text{FeOHPuO}_3^- + 2\text{H}^+$		-10.66	
$>\text{FeOH} + \text{Sr}^{2+} \Leftrightarrow >\text{FeOHSr}^{2+}$	12	2.22 ± 0.13	(17, 32)
$>\text{FeOH} + \text{Sr}^{2+} \Leftrightarrow >\text{FeOSr}^+ + \text{H}^+$		-5.30 ± 0.31	
$>\text{FeOH} + \text{Sr}^{2+} + \text{H}_2\text{O} \Leftrightarrow >\text{FeOSrOH} + 2\text{H}^+$		-14.14 ± 0.40	
$>\text{FeOH} + \text{UO}_2^{2+} + \text{H}_2\text{O} \Leftrightarrow >\text{FeOHUO}_3 + 2\text{H}^+$	17	-3.05 ± 0.43	(33, 34, 35, 36)
$>\text{FeOH} + \text{UO}_2^{2+} \Leftrightarrow >\text{FeOHUO}_2^{2+}$		6.63 ± 0.54	

Table 2. Surface complexation reactions for calcite using the NEM

Reaction	# of Curves Evaluated	logK	Ref.
$>\text{Ca}^{2+} + \text{AmCO}_3^+ \Leftrightarrow >\text{AmCO}_3^+ + \text{Ca}^{2+}$	10 ^a	4.13±0.06	(37)
$>\text{Ca}^{2+} + \text{EuCO}_3^+ \Leftrightarrow >\text{EuCO}_3^+ + \text{Ca}^{2+}$	2 ^a	3.75	(38)
$>\text{Ca}^{2+} + \text{LaCO}_3^+ \Leftrightarrow >\text{LaCO}_3^+ + \text{Ca}^{2+}$	2 ^a	3.24	(38)
$>\text{Ca}^{2+} + \text{NpO}_2^+ \Leftrightarrow >\text{NpO}_2^+ + \text{Ca}^{2+}$	8 ^a	2.35±0.19	(22)
$>\text{Ca}^{2+} + \text{PuO}_2^+ \Leftrightarrow >\text{PuO}_2^+ + \text{Ca}^{2+}$	7 ^a	1.85±0.35	(21)
$>\text{Ca}^{2+} + \text{SmCO}_3^+ \Leftrightarrow >\text{SmCO}_3^+ + \text{Ca}^{2+}$	2 ^a	2.53	(38)
$>\text{Ca}^{2+} + \text{Sr}^{2+} \Leftrightarrow >\text{Sr}^{2+} + \text{Ca}^{2+}$	1	-1.75	(11)
$>\text{Ca}^{2+} + \text{UO}_2^{2+} \Leftrightarrow >\text{UO}_2^{2+} + \text{Ca}^{2+}$	17 ^a	5.12	(14)
$>\text{Ca}^{2+} + \text{YbCO}_3^+ \Leftrightarrow >\text{YbCO}_3^+ + \text{Ca}^{2+}$	2 ^a	1.52	(38)

^a Single point data

Table 3. A comparison of logK data fits for calcite sorption and coprecipitation data^a

Element	Concentration mol/L	Reaction	Species	logK
La	$7 \cdot 10^{-8}$	coprecipitation	LaCO ₃	3.50
	$6.5 \cdot 10^{-7}$	sorption	>LaCO ₃ ⁺	3.24
Sm	$7 \cdot 10^{-8}$	coprecipitation	SmCO ₃	2.53
	$6.5 \cdot 10^{-7}$	sorption	>SmCO ₃ ⁺	3.03
Eu	$7 \cdot 10^{-8}$	coprecipitation	EuCO ₃	3.75
	$6.5 \cdot 10^{-7}$	sorption	>EuCO ₃ ⁺	4.00
Yb	$7 \cdot 10^{-8}$	coprecipitation	YbCO ₃	1.52
	$6.5 \cdot 10^{-7}$	sorption	>YbCO ₃ ⁺	2.38

^a Data from Zhong and Mucci (38). All experiments were open to the atmosphere, in seawater solutions, at identical Ca²⁺ concentrations (0.0177 mol/l), and a pH range of 8±0.5.

Table 4. Simulation of RN partitioning between alluvium and groundwater containing initial RN concentrations of 10^{-8} molal^a

	Iron Oxide	Calcite	Aqueous	Total
	----- log(mol/L) ^b -----			
Americium	n.a. ^c	-8.0	-12.6	-8.0
Europium	-8.0	-9.2	-11.7	-8.0
Neptunium	-8.3	-8.3	-11.2	-8.0
Plutonium ^d	-8.0	-9.2	-10.4	-8.0
Samarium	n.a.	-8.0	-10.9	-8.0
Strontium ^e	-10.1	-12.4	-11.2	-8.0 ^f
Uranium	-8.0	-13.4	-11.7	-8.0

^a 35% porosity; abundance of reactive minerals in Frenchman Flat Alluvium taken from Tompson et al. (5): 1% iron oxide, 1% calcite, 5% smectite, 5% clinoptilolite, and 1% illite/mica (volume percent).

^b Sorbed concentrations expressed as mol/L fluid instead of mol/g mineral to allow for direct comparison to aqueous concentrations.

^c RN-mineral SC reaction constants were not available.

^d Simulations were run assuming oxic environment dominated by Pu(V).

^e Strontium ion exchange to smectite and clinoptilolite is discussed in (5).

^f log(mol/L) for Sr associated with clinoptilolite and smectite are -8.1 and -8.7, respectively.

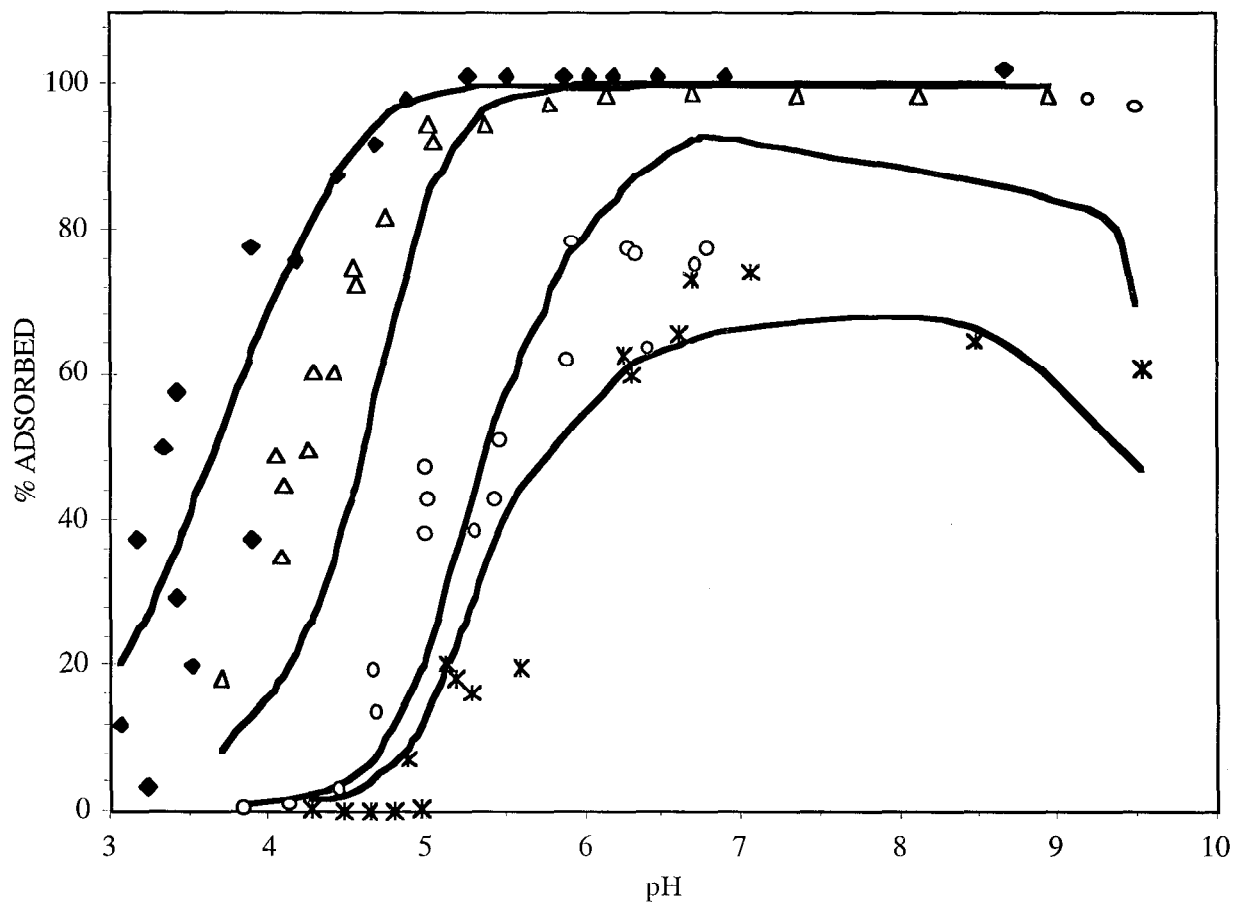


Fig. 1. Sorption of U(VI) on Fe(OH)₃ (600 m²/g) (◆), FeOOH (50 m²/g) (Δ), synthetic Fe₂O₃ (7.2 m²/g) (○), and natural Fe₂O₃ (4.2 m²/g) (*) as a function of pH. Thick line represents data fit using average LogK values. I=0.1, total U(VI)=10⁻⁵ mol/l, 1g solid/L. Data from Hsi and Langmuir (35).

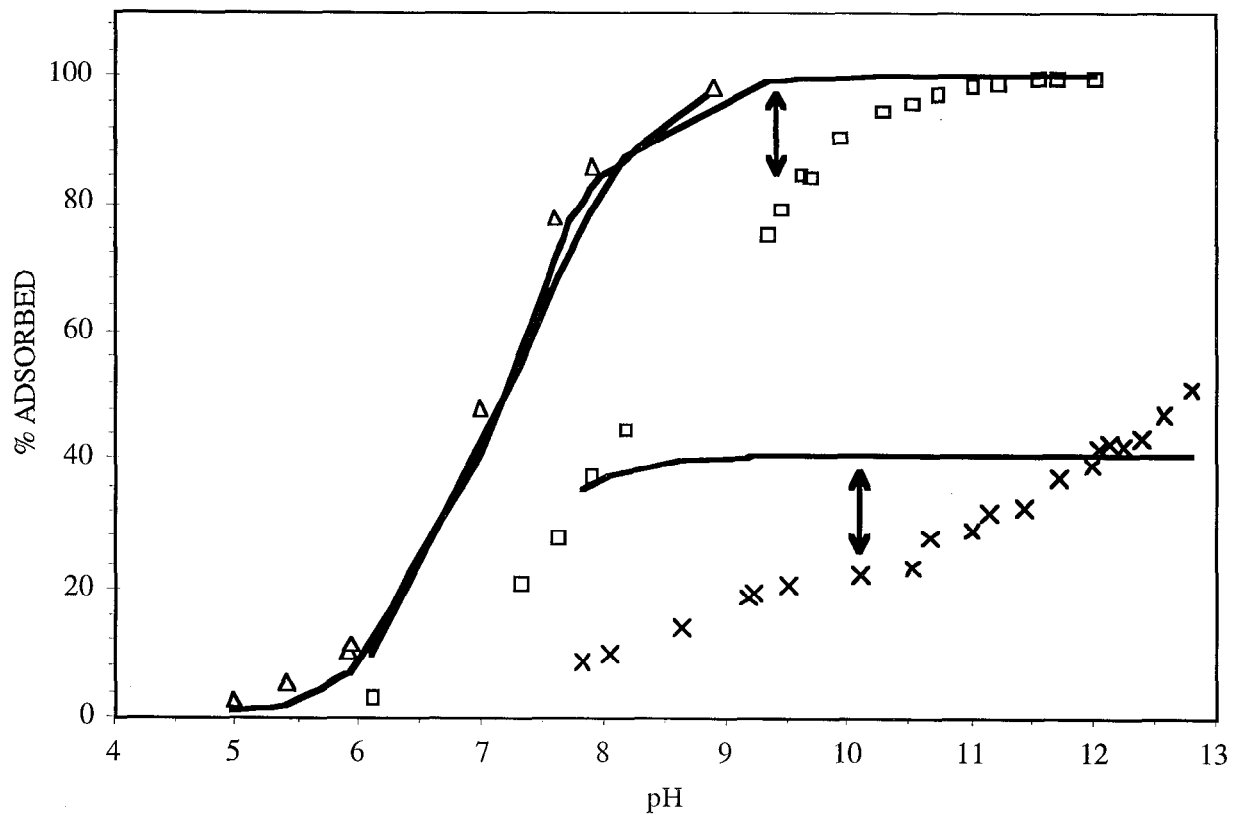


Fig. 2. Sorption of Sr(II) on $\text{Fe}(\text{OH})_3$ as a function of pH at $8.34 \cdot 10^{-6}$ (Δ), $5 \cdot 10^{-3}$ (\square), and $5 \cdot 10^{-2}$ (X) mol/L Sr. Lines represent data fits using average LogK values. $I=1$, 10^{-1} mol/L Fe as $\text{Fe}(\text{OH})_3$, and open to air. Data from Kolarik (17).

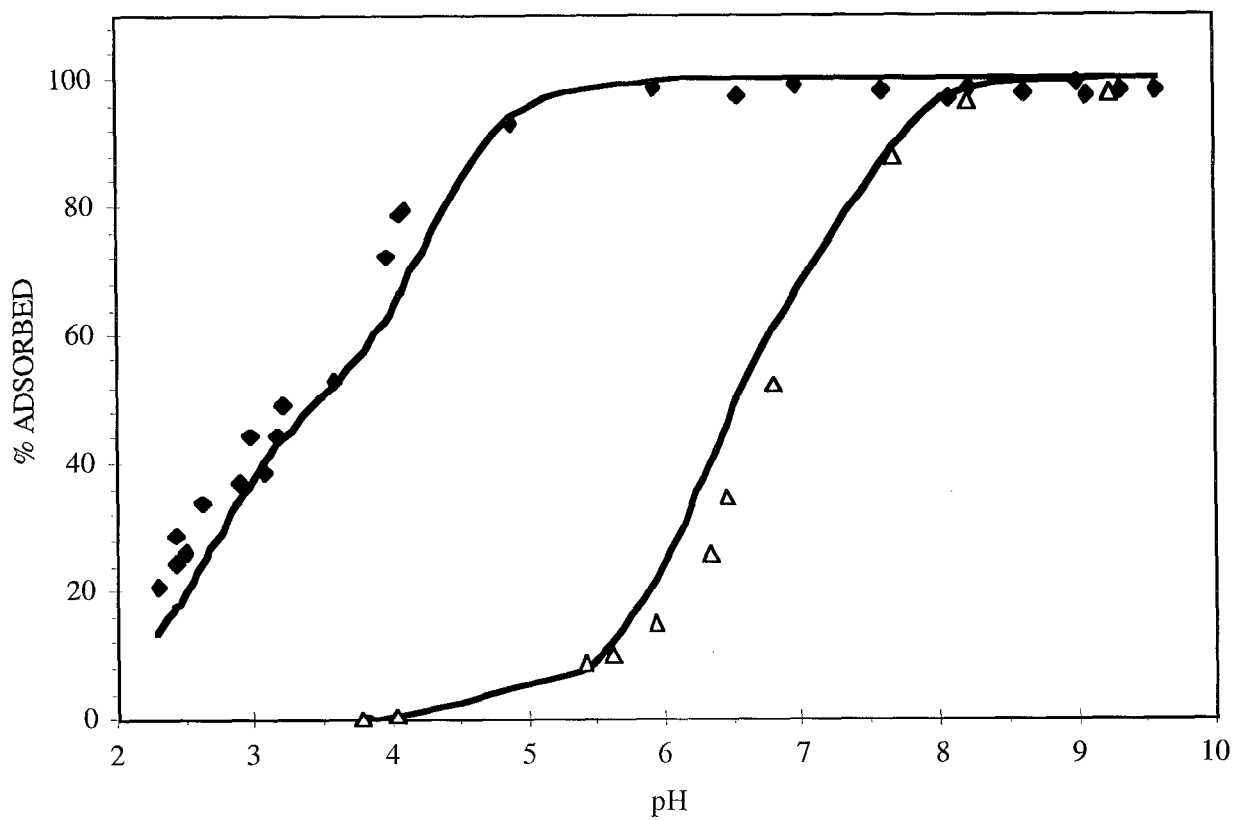


Fig. 3. Sorption of 10^{-11} molar Pu(IV) (◆) and Pu(V) (△) on FeOOH as a function of pH. Lines represent data fit using average logK values. $I=0.1$ and $28.5 \text{ m}^2/\text{L}$ FeOOH. Data from Sanchez et al. (20).

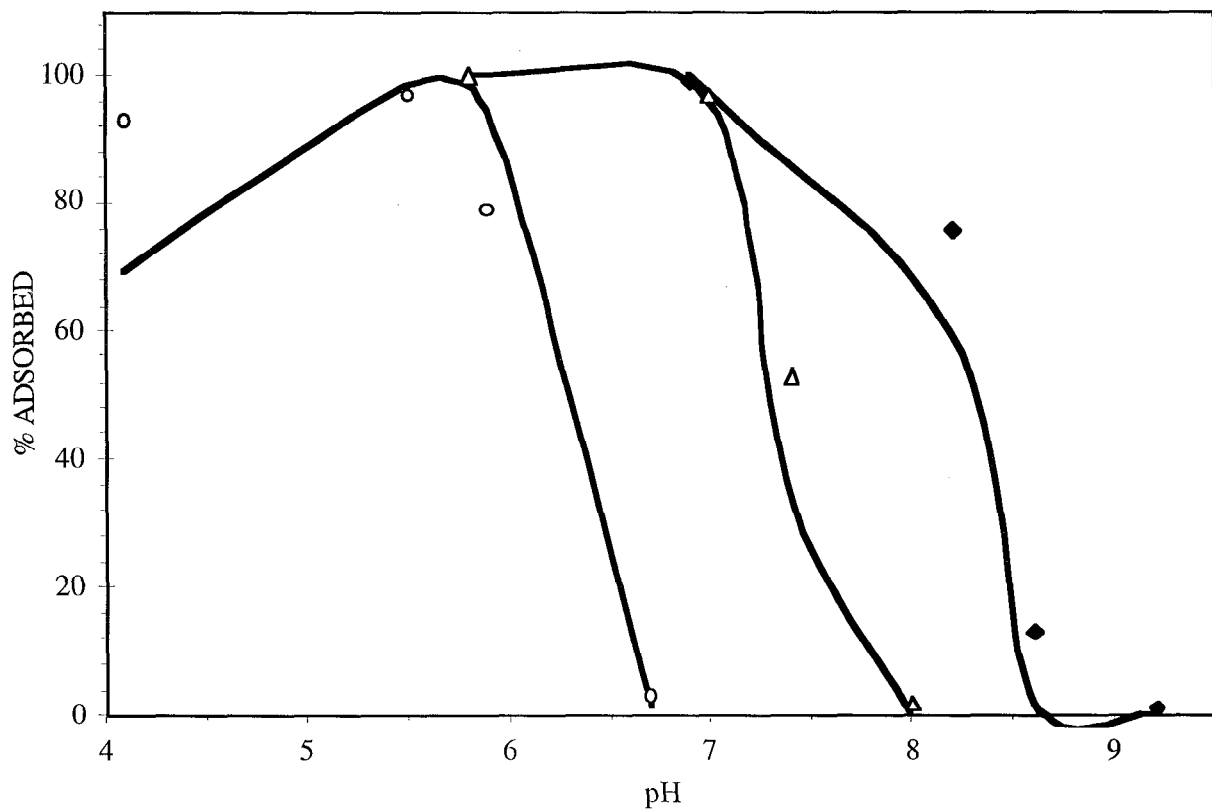


Fig. 4. Sorption of U(VI) on FeOOH as a function of pH at 0.2% (\blacklozenge), 5% (Δ), and 90% (\circ) $\text{CO}_2(\text{g})$ partial pressure. Lines represent data fits using average $\log K$ values. $I=0.1$, $8.4 \cdot 10^{-6}$ mol/L U(VI), 8 g FeOOH/L, and $60 \text{m}^2/\text{g}$ FeOOH. Data from Duff and Amrhein (33).